Oil Shale Solid Waste Recycling in the Development of New Silica Fillers for Elastomeric Composites

CARLOS RENATO PERRUSO,[1] ARNALDO ALCOVER NETO,[2] REINER NEUMANN,[2] REGINA CÉLIA REIS NUNES,[3] MARCUS VINíCIUS DE ARAÚJO FONSECA,[1] REGINA SANDRA VEIGA NASCIMENTO[1]

[1] Instituto de Química/UFRJ, Polo de Xistoquímica, Ilha do Fundão, CT, Bl. A, sala 618, CEP: 21949-900, Rio de Janeiro, RJ, Brazil

[2] Centro de Tecnologia Mineral, Setor de Caracterização Tecnológica, Ilha do Fundão, R. 4, Q. 3, CEP: 21941-590, Rio de Janeiro, RJ, Brazil

[3] Instituto de Macromoléculas/UFRJ, Ilha do Fundão, P.O. Box 68525, CEP 21945-970, Rio de Janeiro, RJ, Brazil

Received 16 June 2000; accepted 17 October 2000

ABSTRACT: The production of Brazilian shale oil gives rise to 6600 ton/day of a solid waste of retorted shale, and larger amounts of dolomitic waste rock are generated during mining. Two vitreous materials were obtained through the melting of different proportions of these two wastes. By leaching these materials with hydrochloric acid at 90°C, two different kinds of silicas (powder and gel, both amorphous) with specific surface areas reaching up to $\sim$ 420 m^2/g were generated. These silicas were further modified through an Ostwald-ripening type of treatment in ammonium hydroxide solution at 80°C. The process eliminated almost completely the deleterious micropores. The obtained silicas were evaluated as reinforcing fillers for SBR-1502. The employment of one of the modified silicas gave rise to a composite with better mechanical properties than those displayed by the one with untreated silica. Scanning electronic microscopic observation disclosed the existence of great morphological differences between these silicas. Apparently, the aging treatment gave rise to the production of better anchoring sites for the elastomer molecules. NMR studies also showed the reduction of the silanol content of the treated silica. The fracture surface of the composite disclosed a good wetting of this silica by the elastomeric matrix. © 2001 John Wiley & Sons, Inc. J Appl Polym Sci 81: 2856–2867, 2001

Key words: SBR; silica; Ostwald ripening; surface modification; wetting

INTRODUCTION

The process for the production of shale oil (an alternative raw material similar to petroleum) is responsible for the generation of large amounts of solid waste. The retorting of oil shale by Petrobras in Brazil produces about 2.4 million tons per year of retorted shale, a solid waste that represents about 80 or 90% of the feeding raw material of the process.[1] During the mining step, a dolomitic layer present in the geological formation is also processed and gives rise to even larger amounts of waste rock. The disposal of large amounts of waste poses an environmental and technical problem. Therefore, it would be highly

Correspondence to: R. C. R. Nunes.

Contract grant sponsors: Ministério de Ciência e Tecnologia; Conselho Nacional de Desenvolvimento Científico e Tecnológico; Financiadora de Estudos e Projetos; Fundação Universitária José Bonifácio; Programa de Núcleos de Excelência.

Journal of Applied Polymer Science, Vol. 81, 2856–2867 (2001)

desirable to find ways of recycling these materials.

The two wastes produced, the retorted oil shale (hereafter called RS) and the top fraction of the dolomitic layer (hereafter called TDL), were used for the development of glasses and glass ceramics.[2] Other researchers have also used similar oil shale wastes for the same purpose.[3,4]

However, depending on the composition, the developed glasses presented a poor chemical durability in different media. Thus, a new focus was given, devoted to the possibility of the development of silicas from these glasses.[5] This idea is based on the theory developed by Huggins et al.[6] that accounts for the durability of glasses in accordance with the number of bridging oxygens in the network structure by calculating the ratio of silicon to oxygen atoms. In SiO_2, the relation is maximal 1 : 2, or 0.5. In Na_4SiO_4, it is 1 : 4, or 0.25. Thus, by introducing cations into the silica network, the ratio of silicon to oxygen atoms decreases. The presence of monovalent cations in the silica network causes a rupture of the structure, increased fusibility, decreased viscosity, and reduced chemical durability and thermal endurance. Hence, a tetrahedral SiO_4 unit can either be bound by all of its oxygen atoms to other silicon tetrahedra or it may have one, two, or three of its corners occupied by nonbridging oxygens bound to other modifying cations. The amount of nonbridging oxygens affects the polymerization, the spatial arrangement, and thus also the properties of glass. The formula developed by Huggins et al. to account for the Si/O ratio is shown in eq. (1), for any given composition of glass:

$$\mathrm{Si/O} = \frac{\mathrm{SiO_2}/100}{\mathrm{mol SiO_2} \sum [(\mathrm{M}_m\mathrm{O}_n/100)(\mathrm{O}_n/\mathrm{mol M}_m\mathrm{O}_n)]} \quad (1)$$

where SiO_2 is the weight percentage of SiO_2; mol SiO_2 is the molecular weight of SiO_2; M_mO_n is the weight percentage of each oxide, including SiO_2; mol M_mO_n is the molecular weight of each oxide; and O_n is the number of oxygen atoms in the oxide.

The great majority of the known technical glasses that are commercially used are chemically resistant, because they present solid structures that are resultant from Si/O ratios > 0.4, corresponding to an average number of bridging oxygens of about 3. Conversely, it is interesting to note that for an Si/O ratio of 0.286, the number of bridging oxygen atoms is about 1, and for a ratio of 0.333 this number is about 2. These are undoubtedly extreme limits of connectivity in the glass network. On the basis of this approach, we decided to develop the different compositions of the glasses that could be produced from the mentioned wastes. In this work we are synthesizing glassy materials that possess a low number of bridging oxygens, precisely in the limits of 1 and 2, which should behave differently when submitted to acid leaching for the development of new silicas.

Since the early years of the rubber industry, particulate fillers and pigments were added to rubber for many reasons. Fillers are used in rubber reinforcement and also to reduce cost, produce color, increase density, and improve processing. Reinforcement of rubber is a very important area of rubber compounding technology, as, for example, in the use of fillers in tread and sidewall of tires used to improve performance and service life. Carbon black is undoubtedly the most reinforcing filler for rubber with regard to the diversity of its physicochemical characteristics as well as to the level of performance that may be achieved. However, there is a general trend to replace carbon black with white mineral fillers, such as silica. This one, which produces materials with worse mechanical properties than those produced with carbon black, has had its use restricted for a long time. Because of a better knowledge of the reinforcement phenomena, it has been increasingly used in technical goods.

The great disadvantage of using silica instead of carbon black is its poor interaction with the polymeric matrix, because of the polar nature of its fully hydroxylated surface. To overcome this situation, some organofunctional silane-coupling agents were employed.[7] In some cases, these silanes appear to equalize the reinforcing ability of silicas and carbon black, but its widespread use is limited by cost factors.

In tire applications, synthetic silicas are employed mainly in the form of precipitated silicas to act as reinforcing fillers.[8] In fact they act as reducing rolling resistance and to improve mileage and wet traction. The key to the improvements is in the use of silica instead of carbon black as the reinforcing filler.[9]

In applications such as rubber reinforcement, the organization of the silica structure and the chemical bond repartition (siloxane bridges and silanols) are very important factors. To control and modify these properties, it is necessary to

study the surface of this material and particularly to determine the properties of the hydroxyl sites, which may be classified as single and geminal silanols.[10] To make a distinction between these sites and the siloxane bridges, it is necessary to analyze the ability of the surface to interact with molecular chains. Solid-state nuclear magnetic resonance (NMR) was used to identify the site occupancies.[11,12]

To change silica characteristics and properties, the Ostwald-ripening process may be used. It affects the amount of hydroxyl groups on the surface because it is driven by differences in surface energy.[13] Different silicon sites may appear and disappear, mainly as a result of the condensation of silanols and the rupture of siloxane bridges. This process is especially important at pH near 9–10 or even higher, where the hydroxide ions catalyze the dissolution and deposition of silica.[14] A distinction between silanols and siloxane bridges may be achieved through the use the solid-state ^{29}Si-NMR technique coupled with magic angle spinning (MAS). Quantitative information may be provided with MAS, calculating the fractional population of silanol sites, f_s, defined in eq. (2)[15]:

$$f_s = \frac{\text{geminal} + \text{single}}{\text{geminal} + \text{single} + \text{siloxane}} \qquad (2)$$

which is determined through the relative peak areas of the various signals in the MAS/NMR spectra.

In this work we are looking for new processes of producing silica from solid wastes, and for a simple modification process for these silicas, to improve ultimate failure properties in styrene butadiene rubber (SBR) formulations.

MATERIALS AND METHODS

Si/O Ratio Calculation

The Si/O ratios were predicted for all the batches by using the formula of Huggins et al.[6] The ratios were recalculated after the chemical analysis of the synthesized glasses.

Glass Production

The two wastes from oil shale processing (RS and TDL) were individually ball milled and classified by sieving until all the samples presented a particle size < 175 μm. After that, appropriate weights of RS (50 or 20% of the mixture, accordingly with the Si/O ratio intended) and TDL (50 or 80% of the mixture, respectively) were added to a ball mill (with only a few balls to improve mixing without producing milling) and mixed for 1 h. The two mixtures were melted individually in a graphite crucible (batches of 20 kg) at a constant temperature of $\sim$ 1550°C in an electric induction furnace for 1 h. The melt was poured into a water container to prepare a frit, which was subsequently dried in an oven at 110°C for 24 h. After that, the frit was ball milled and classified by sieving until all the particles presented a size < 105 μm. The two glasses produced from the melt of the mixtures 50% RS/50% TDL and 20% RS/80% TDL were designated G55 and G28, respectively.

Glass Leaching

Batches of 500 g of glass were added to 4 L of 6*N* hydrochloric acid, previously stabilized at (90 $\pm$ 2)°C, in a 6-L Pyrex® glass reactor. The leaching reactions were conducted for 6 h under mechanical stirring, as determined by kinetic measurements.[16] The leaching of G55 and G28 yielded the silicas S55 and S28, respectively

Washing

After leaching, the reaction medium was cooled and drained inside a closed system to a vacuum filter. The silica produced was filtered and rinsed with distilled water. The process was repeated once more to eliminate the yellowish coloration of the solution, which is due to the presence of ferric ions. The silicas developed from the glasses G55 and G28 as described were designated S55A and S28A, respectively.

Drying

After processing, the resulting silicas were left to dry in an oven at 110°C for 24 h.

Milling

The silicas were ball milled for 12 h for reduction of particle size in a 5.5-L capacity standard laboratory mill in batches of about 3 kg of sample for a volume of balls of about 1.5 L.

Neutralization

The pH of part of the silicas was adjusted to 7.5 by potentiometric titration with a diluted ammo-

nium hydroxide solution under mechanical stirring, yielding the silicas S55N and S28N. The system was allowed to reach the equilibrium for 1 h in the selected pH.

Aging Treatment

Modification of the silicas S55N and S28N was performed under an Ostwald-ripening-type process, conducted in 2*N* ammonium hydroxide for 16 days at 80°C in a Pyrex® glass reactor inside a water bath. These suitable conditions imparted the greatest structural changes in the silicas and were selected from a set of experiments previously performed.[17]

Washing, Neutralization, and Drying

After aging, the silicas were vacuum filtered and washed with distilled water. The pH of the silicas surface was adjusted to 7.5 (as described before), yielding the silicas S55MN and S28MN after drying in an oven at 110°C for 24 h. The silicas were observed in the SEM before and after aging.

Milling

Part of the silicas S55MN and S28MN was ball milled for 48 h, aiming a further reduction of particle size. This procedure yielded the silicas S55MNC and S28MNC.

BET Surface Area

Specific surface area analyses were performed in a Micromeritics ASAP 2010 instrument following the BET method.[18] The silica samples were heated to 300°C under vacuum before measurements.

Particle Size Distribution

Samples were dispersed in distilled/demineralized water for analysis in a Micromeritics sedigraph 5100 (Stokes law), in the range of 40 to 0.5 μm.

XRD

X-ray diffraction (XRD) analysis was conducted by the powder method in a Siemens/Bruker AXS instrument, model D5005, with parallel geometry and Goebel mirror by using CuK_{α} radiation (λ = 1.54184 Å; 40 kV; 40 mA) and proportional detector.

Table I Mixes Formulations

Components	phr
SBR-1502	100.0
Silica	Variable
Zinc oxide	2.50
Stearic acid	2.00
Poly(ethylene glycol) 4000	2.50
Mineral oil	10.00
Sulfur	2.00
TMTD[a]	1.00

[a] Tetramethyl thiuram disulfide.

NMR Measurements

Solid-state ^{29}Si-NMR experiments were carried out in a Bruker Avance DRX 300 spectrometer at 7.05 T. MAS was carried out at 5-kHz spinning rates.

SEM/EDX

Scanning electron microscopy analysis was conducted in a Leica S440 instrument coupled to an Oxford Link ISIS L300 Energy Dispersive X-ray (EDX) analyzer operated at 20 kV, using a solid-state detector with a resolution of 133 eV at 5.9 keV. All samples were sputter coated with gold under vacuum prior to observation.

Mix Formulation

The materials and additives used in the mixes are given in Table I: SBR-1502, a styrene butadiene rubber, containing 22.8% styrene (Petroflex, Brazil); silica Zeosil® 175 used without modification for comparison (Rhodia, Brazil); zinc oxide (Vetec, Brazil); stearic acid (Rhos, Brazil; reagent grade); polyethylene glycol 4000 (Vetec, Brazil; reagent grade); mineral oil (Irwin, Brazil; reagent grade); sulfur (Carlo Erba, Brazil); and tetramethyl thiuram disulphide, TMTD (Monsanto). All silicas were dried at 110°C for 24 h prior to use in SBR formulations. Mixing was carried out in a two-roll mill at 50°C, according to ASTM D 3191. The mixes were designated in accordance with their type and quantity of silica employed (in phr, parts per hundred parts of resin). Thus, SBR-S55A/50 stands for a mix with the silica S55A at a concentration level of 50 phr. Optimum cure time at 150°C was obtained from a Monsanto rheometer. Mixes were vulcanized in a heated press at 150°C

Table II Chemical Composition of the Wastes and Glasses

Component	RS (%)	TDL (%)	G28 (%)	G55 (%)
SiO_2	51.5	19.7	40.3	54.3
Al_2O_3	11.8	1.9	5.2	9.4
Fe_2O_3	6.3	1.3	1.1	0.35
FeO	1.8	1.9	2.3	0.91
TiO_2	0.73	0.10	0.31	0.52
MgO	2.0	14.9	17.3	12.3
CaO	2.8	21.6	28.1	18.5
K_2O	3.2	0.24	1.3	2.3
Na_2O	1.4	0.27	0.95	1.4
Loss on ignition (1000°C)	18.4	36.5	—	0.19
Total	99.9	98.4	96.9	100.2
Si/O ratio	—	—	0.27	0.32
Number of bridging oxygens	—	—	~ 1	~ 2

and 3.1 MPa. Vulcanizates were conditioned for 24 h, according to ASTM D3182, prior to testing.

Mechanical Testing

Mechanical properties were measured along the grain direction. Stress–strain data were obtained from an Instron dynamometer, Model 4204, by using an ASTM C-type dumbbell specimen, according to ASTM D 412. Tensile fractured surfaces were observed in the SEM microscope.

RESULTS AND DISCUSSION

The chemical compositions of the wastes, RS and TDL, and the glasses, G55 and G28, are shown in Table II. The Si/O ratio calculated for the glasses and the corresponding number of bridging oxygens are also presented in this table. It is interesting to note the main differences between the two wastes. RS is rich in silicon and aluminum oxides, whereas TDL is rich in calcium and magnesium oxides, allowing the Si/O ratio to be controlled through the melt of different proportions of these two wastes. The Si/O ratio may broadly be considered as a measure of the polymerization degree of a glass network.[19] As expected, G28 presented a very low number of bridging oxygens. This suggests that this glassy material would be less resistant through an acid-leaching process. In fact, the result was the complete failure of the network as a consequence of the low number of bridging oxygens. By this manner, G28 was completely dissolved and gave rise to a homogeneous translucent gel of silica S28, which completely filled the leaching solution volume. The gel obtained presented a yellowish coloration as a result of the presence of ferric ions. The removal of cations through washing with distilled water yielded a colorless gel. The glass G55 has shown a completely different behavior. The leaching process did not produce any observable morphological changes in the silica S55. In accordance with the Huggins et al. theory, this is a consequence of the number of bridging oxygens of this glassy material, which is about two, indicating the existence of a sufficient degree of polymerization to hold the structure together.

The processes of production of silica in aqueous media (precipitated silica) for the rubber industry usually involves the acidification of sodium silicate solutions. Differently, with the new process of production of silica presented, we propose that interesting results may be achieved through the control of the leaching kinetics and processing conditions for the application of the homogeneous translucent gel in precipitation or in sol-gel-like processes.

XRD patterns confirmed the noncrystalline nature of the materials obtained after melting. The silicas developed presented the same behavior and XRD patterns may be seen in Figure 1. The process of leaching did not produce any kind of restructuring or crystallization.

SEM images of the silicas after neutralization and drying, S55N and S28N, may be seen in Figure 2(A) and (C), respectively. These silicas are very different: S55N showed smooth surfaces, characteristic of brittle fractures of the original milled glass particles, the shapes of which remained intact after leaching; S28N showed a gel-type morphology, completely different from the original glass particles. These results are in perfect agreement with the behavior of the glasses during leaching, as expected from their Si/O ratio.

EDX and chemical analysis confirmed that the leaching was complete for both silicas, showing a final composition of 99.9% SiO_2. No other than silicon cations were detected down to the detection limit of about 0.05% by weight.

The hydrochloric acid was recovered through atmospheric distillation of the leaching liquor in quite large proportions, about 75% at a concentration of 4.8*N*, showing that the recycling pro-

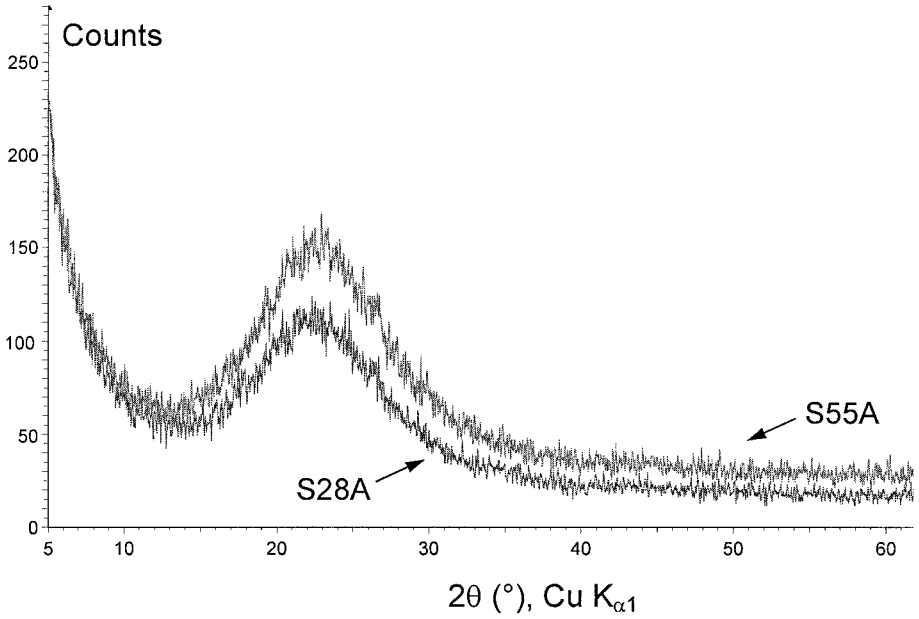

Figure 1 XRD patterns of the silicas S55A and S28A.

cess of the acid used in the leaching experiments is possible and practical. It is also important to consider that the distillation residue is rich in calcium and magnesium and may be useful for agricultural applications. The possibility of reusing the acid without distillation is another option

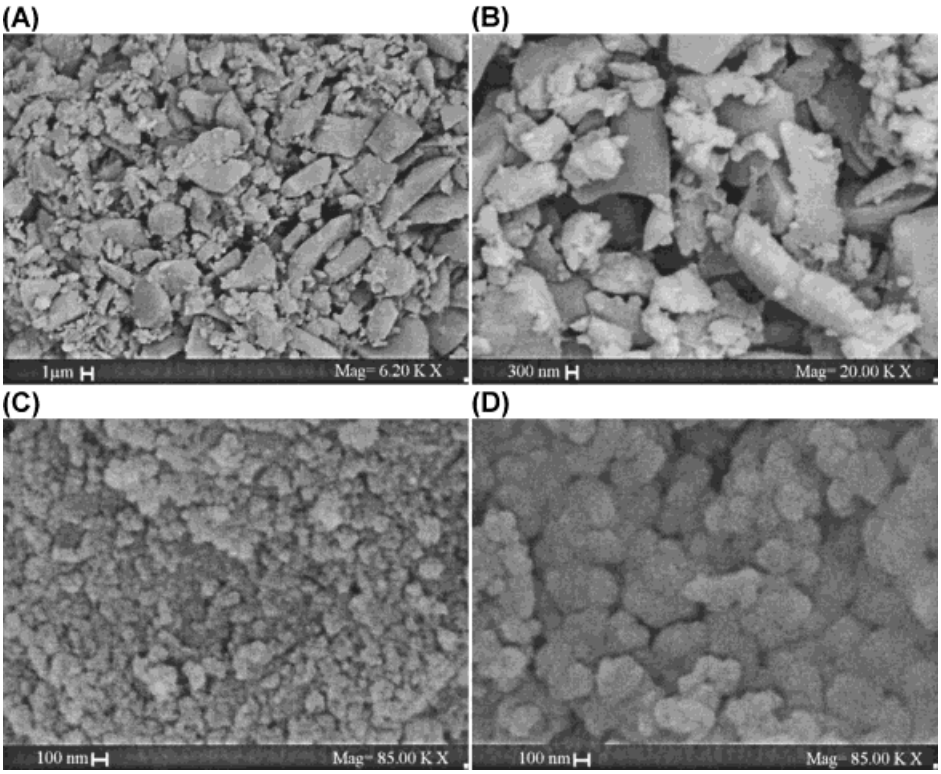

Figure 2 SEM images showing morphology (roughness) of the surface before and after treatment: (A) S55N; (B) S55MN; (C) S28N; (D) S28MN.

Table III Physical Characteristics of Silicas

Silica Type	Area (m^2/g)	Micropores Vol. (mL/g)	pH	Density (g/cm^3)	Average Particle Size (μm)[a]
S55A	332	0.170	4.0	1.892	5.04
S55N	319	0.167	7.5	1.937	5.04
S55MN	87.5	0.0375	7.5	2.041	5.08
S55MNC	95.3	0.0399	7.5	2.095	2.47
S28A	357	0.140	4.0	2.087	3.21
S28N	344	0.133	7.5	2.121	3.21
S28MN	81	0.0369	7.5	2.181	3.28
S28MNC	86	0.0389	7.5	2.197	2.66
Z175[b]	186	0.0012	6.0	2.209	< 0.5[b]

[a] Calculated by the Sedigraph, except Z175, estimated by SEM.
[b] Z175, silica Zeosil® 175.

that may not be discarded, but in this case, each ion concentration cycle must be evaluated.

The physical characteristics of all silicas employed with the elastomer may be seen in Table III. The silicas obtained presented different physical properties. The acidic forms, S55A and S28A, presented the highest specific surface areas, and consequencely, the highest volume of micropores. After neutralization, the silicas S55N and S28N presented a pH of 7.5 and only small changes on the other properties. After the aging treatment, the silicas were designated as S55MN and S28MN and presented a great reduction in specific surface area and in the volume of micropore. After additional ball milling, the silicas were designated as S55MNC and S28MNC and presented mainly a reduction in average particle size. Also in Table III, the silica Z175 (silica Zeosil® 175), without any kind of treatment, was used for comparison in the rubber. Figure 2 shows the effect on the morphology (roughness) of the particles promoted by the Ostwald-ripening treatment. S55N [Fig. 2(A)] yielded S55MN [Fig. 2(B)], which does not show any changes produced by the treatment (seen at different magnifications), and S28N [Fig. 2(C)] yielded S28MN [Fig. 2(D)], exhibiting a great morphological change (seen at the same magnification). Ostwald ripening may induce that kind of effect driven by the differences in solubility of the silica particles of different curvature radii. The conditions selected for the process allow the existence of concentrations as high as 1000 ppm of silica in the solution or higher, and the hydroxide ions catalyze the dissolution and precipitation reactions. Thus, the small primary particles disappear as a result of having a greater solubility; in parallel, the larger ones grow at the expense of the small ones. We must also consider the great reduction in micropore volumes. Because these pores are very small regions with negative radii of curvature, they possess the lowest solubility relative to the other surfaces of silica (larger pores, flat surfaces, and particles with positive radii of curvature) and deposition occurs predominantly on those places. This accounts for the reduction of micropore volumes and also the corresponding specific surface area.

The process is also followed by changes in the surface silanol concentration, as can be seen in Table IV, calculated from the spectra presented in Figure 3 (Gaussian lines were used in curve fitting). Solid-state ^{29}Si-MAS/NMR data showed the reduction of the fractional population of silanol sites of the silicas after treatment, S55MN [Fig. 3(B)] and S28MN [Fig. 3(D)]. This probably occurs as a net result of a greater number of silanol condensation reactions than siloxane bond breakage, the same reason that gives rise to the filling of micropores with silica and the reduction of specific surface area.

As can be seen in Figure 4, the rheometer curves indicate that all different types of silica

Table IV Fractional Population of Silanol Sites of the Silicas, f_s, Before (N-type silica) and After (MN-type) the Aging Treatment

Silica	f_s (%)
S55N	43.53
S55MN	33.59
S28N	44.93
S28MN	37.47

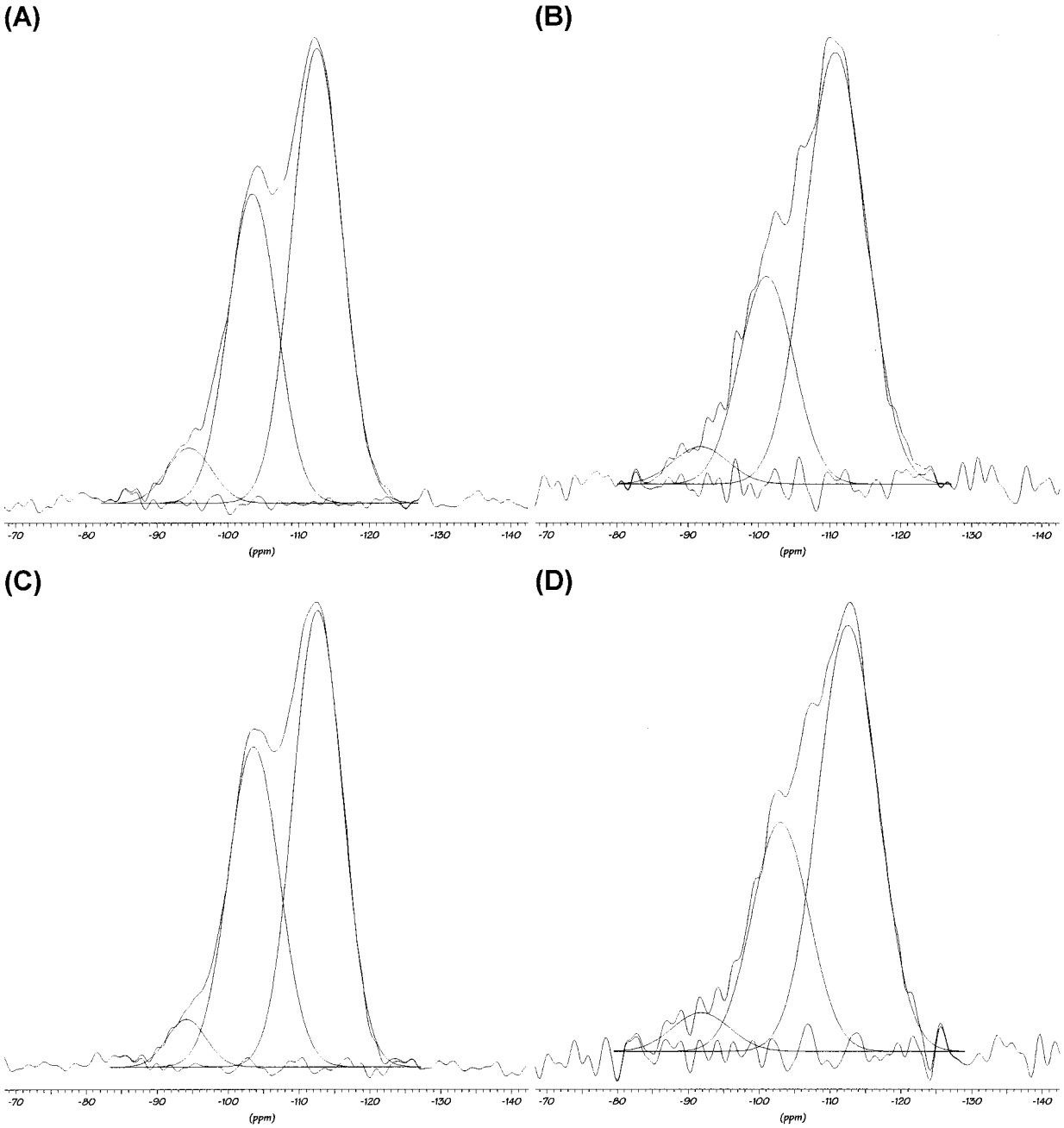

Figure 3 Solid-state ^{29}Si-MAS/NMR spectra of the silicas before and after treatment: (A) S55N; (B) S55MN; (C) S28N; (D) S28MN. Chemical shifts are presented in ppm from tetramethylsilane. Curve fitting was performed using Gaussians.

obtained had a quite marked effect on the rubber-cure behavior. The physical adsorption activity of the filler surface is of much greater importance than its chemical nature for the mechanical properties of the vulcanizates.[20] However, chemical surface groups play an important role on the rate of cure with many vulcanizing systems, depending on the pH level of these groups. Thus, when acidic fillers are used in compounding with rubber, it is necessary to add neutralizing agents such as amines or glycols to overcome their retardation effect on the cure rate. Thus, the acidic forms of the silicas, S55A and S28A, yielded the worst final materials after rheometry and were not submitted to mechanical tests. In the mix SBR-S28A/50, the cure was not attained after the

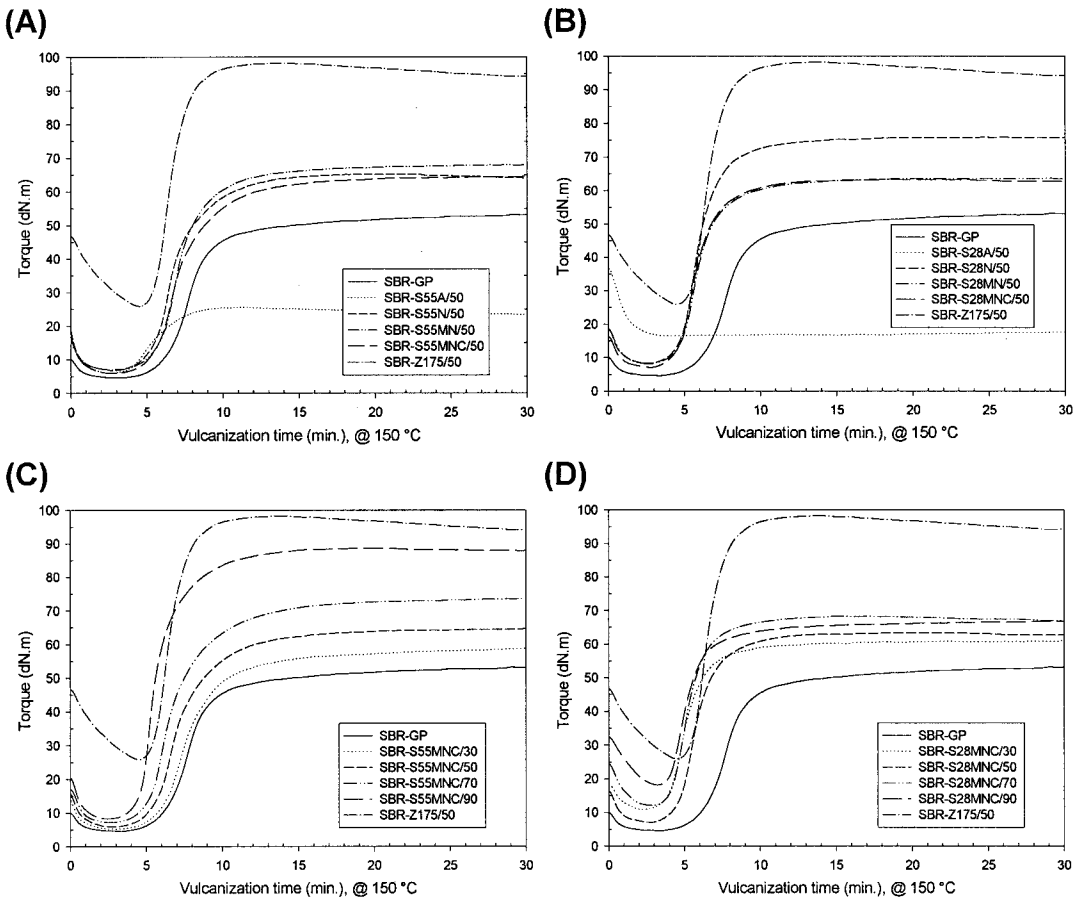

Figure 4 Reographs of silica–SBR mixes: (A) and (B), at 50 phr for all silicas; (C) and (D), at variable concentration of MNC-type silicas.

end of the experiment time, 30 min. The N, MN, and MNC types of silica seem to affect cure in a very similar way, producing vulcanizates in a few minutes, as can be seen in Figure 4. The simple neutralization process adopted seems to be very suitable in achieving cure at a reasonable time.

The physicomechanical properties of the vulcanizates may be seen in Table V. The ultimate failure properties of the vulcanizates SBR-S55MN/50 and SBR-S55MNC/50 were very similar to the ones obtained for SBR-S55N/50. It is also interesting to note that a small reduction in the average particle size did not affect mechanical properties in this set. However, the vulcanizates SBR-S28MN/50 and SBR-S28MNC/50 have shown an improvement in ultimate failure properties in comparison with SBR-S28N/50. As discussed later, in both types of silica systems, S55 and S28, the specific surface areas and the micropore volumes were reduced after the aging treatment. Thus, it may be deduced that the small improvement in mechanical properties of the vulcanizates comes from the morphological changes produced on the surface of the S28MN silica sample after aging in ammonium hydroxide. It is also important to remember the small reduction in the fractional population of silanol sites imparted to this silica, which may permit a better interaction between the silica and the polymeric matrix. Figure 5 shows SEM images of the tensile fractured surfaces of some SBR mixes. In SBR-S55MN/50, a great number of debonded silica particles seems to indicate a poor filler–polymer interaction, as in SBR-S55N/50 (not shown). In Figure 5(A), on the left, backscattered electron image, and, on the right, the same on secondary electron image, shows through different contrasts the poor interaction between the silica S55MN and the polymer. On the right, the SBR-S28MN/50 formulation presented a different behavior, because the adhesion degree at the interface seems to be better than for the SBR-S28N/50 formulation. It is interesting to correlate this information with the data presented before. The changes imparted to

Table V Physicomechanical Properties of Vulcanizates

Vulcanizate[a]	Tensile Strength (MPa)	100% Modulus (MPa)	Elongation at Break (%)	Rupture Energy (J)
SBR-GP[a]	1.22	0.552	413	1.03
SBR-S55A/50	—[b]	—	—	—
SBR-S55N/50	2.15	0.859	894	3.71
SBR-S55MN/50	2.03	0.903	734	2.93
SBR-S55MNC/30	1.90	0.689	712	2.76
SBR-S55MNC/50	2.43	0.820	799	4.17
SBR-S55MNC/70	2.91	0.954	862	5.02
SBR-S55MNC/90	3.91	1.229	852	7.35
SBR-S28A/50	—[b]	—	—	—
SBR-S28N/50	3.69	1.11	846	6.35
SBR-S28MN/50	4.21	0.880	1153	7.97
SBR-S28MNC/30	2.72	0.760	738	3.82
SBR-S28MNC/50	4.15	0.847	1167	7.76
SBR-S28MNC/70	6.95	1.095	1431	17.30
SBR-S28MNC/90	6.99	1.329	1322	17.42
SBR-Z175/50	13.87	1.29	1426	25.57

[a] For each vulcanizate "/XX" means the concentration of the respective silica in phr. SBR-GP, pure rubber.
[b] Not tested.

the corresponding silica after treatment (S28MN) gives rise to a structure with higher primary particles, as shown in Figure 2(D). In parallel, this also makes the cavities (voids or pores) between the primary particles larger. The main part of them may be classified in the range of mesopores (2–20 nm in diameter) and macropores (20–60 nm in diameter). These are the most frequently distributed pore sizes in primary aggregates (constituted of primary particles); they are especially important for rubber reinforcement because of their strong interaction with polymer molecules during the mixing procedure in the roll mill, as a result of strong mechanical forces and temperature. This structure (voids and pores) formed by the three-dimensional structure of the silicas has a great effect on rubber properties. In this case the changes in structure observed in the S28-type silica after aging seems to have improved the performance of the final vulcanizate, because the treatment gave rise to better anchoring sites for the elastomer molecules.

The effect of the filler loading also may be seen in Table V, for the silicas S55MNC and S28MNC. It is easy to see the better performance exhibited by the vulcanizates filled with the S28-type silica. The energy at rupture is generally accepted as the best single criterion for reinforcement and can be obtained from the stress–strain curve as the area between the curve and the elongation axis. According to this criterion, all silicas imparted reinforcement to the vulcanizates relative to the unfilled vulcanizate (SBR-GP). However, looking at Figure 6, the difference between the two types of treated silica is evident. The silica S28MNC gave rise to a higher reinforcement level, reaching a maximum at about 17 J, for filler loading in the range of 70 to 90 phr. Beyond this point, a volume dilution factor may take place (filler acts as diluent), and the vulcanizate properties again deteriorate, because there not will be enough rubber matrix to hold the fillers. For the silica S55MNC, as a result of their lower interaction with the matrix, it seems that this point was not reached yet.

CONCLUSION

A new process for the production of silica was developed. Two different silicas were produced with different physical properties and nature: one of a powder type, and the other of a gel type. The two silica types, S55 (powder type) and S28 (gel type), seem to behave differently as fillers for SBR formulations. The aging treatment in ammonium hydroxide of the powder-type silica did not impart any improvement on the ultimate failure proper-

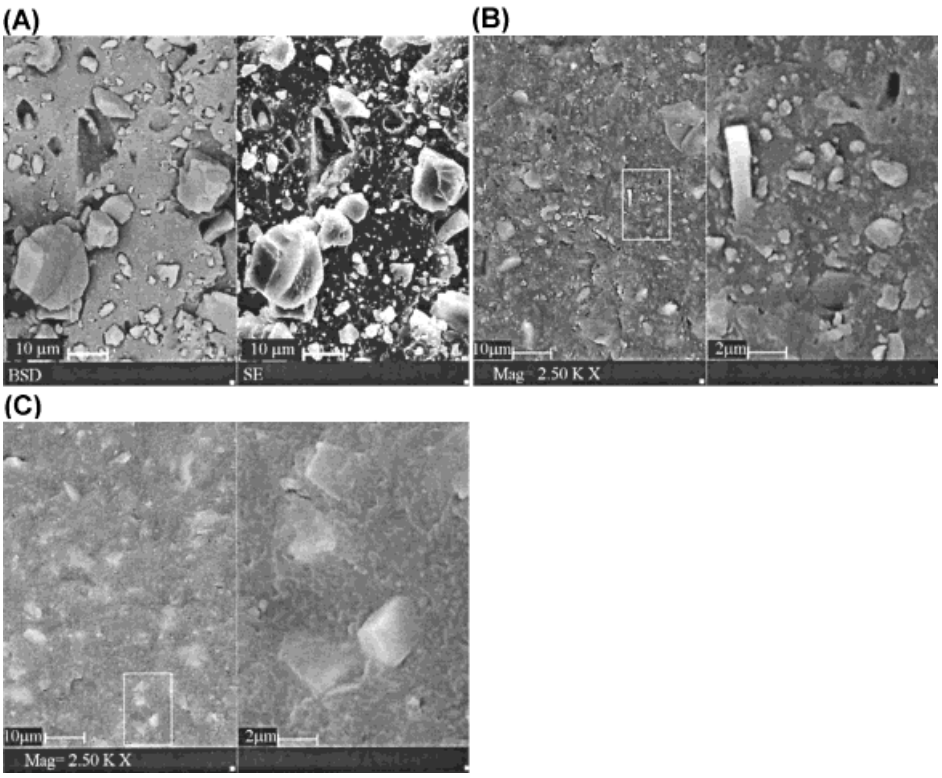

Figure 5 SEM images showing tensile fracture surfaces of some silica–SBR formulations: (A) SBR-S55MN/50 observed by backscattered (left) and secondary electrons (right); (B) SBR-S28N/50; (C) SBR-S28MN/50.

ties of the SBR vulcanizates (particles remained debonded). The gel-type silica behaved in a different way and after treatment produced materials with slightly better properties. SEM images showed unambiguously the great morphological changes imparted to the gel-type silica as a result of the aging treatment. This process seems to be a valuable tool in morphology and physical properties tailoring. These morphological changes together with a small reduction in the fractional

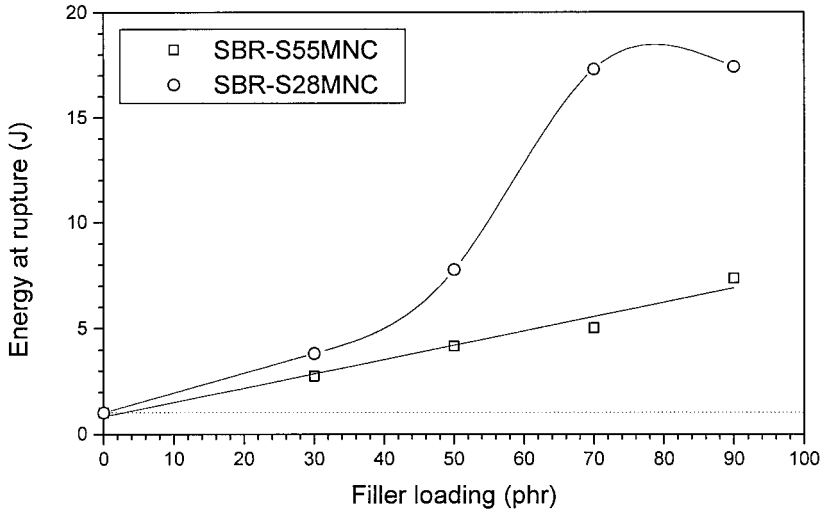

Figure 6 Energy at rupture curves. Filler loading expressed in phr.

population of silanol sites may be responsible for the development of better anchoring sites for the elastomer molecules. In the same way, an improved adhesion degree seems to be supported by the SEM images shown on the tensile fracture surfaces (particles seem to be wetted). As the aging treatment is very simple and almost costless, it seems to be promising for the modification of the surface properties of silicas, and further studies are in progress aiming to evaluate new materials with the partial replacement of high-cost commercial silicas in the vulcanizates.

The authors thank the Ministério de Ciência e Tecnologia (MCT), Conselho Nacional de Desenvolvimento Científico e Tecnológico (CNPq), Financiadora de Estudos e Projetos (FINEP), Fundação Universitária José Bonifácio (FUJB), and the Programa de Núcleos de Excelência (PRONEX) for financial support. Also, the authors thank the Instituto Nacional de Tecnologia (INT) for the rheometry analysis and the Instituto de Macromoléculas Professora Eloisa Mano (IMA/UFRJ) for the vulcanization and the mechanical tests.

REFERENCES

1. Petrobras, Boletim Informativo; Incubadora Tecnológica de São Mateus do Sul: Paraná, 1998; p 6.
2. Fonseca, M. V. A. D.Sc. Thesis, USP, São Paulo, 1990.
3. Shelestak, L. J.; Chavez, R. A.; MacKenzie, J. D.; Dunn, B. J Non-Cryst Solids 1978, 27, 83.
4. Horiuchi, T.; Mizuno, T.; Chung, C. H.; MacKenzie, J. D. Proceedings of the Mineral Waste Utilization Symposium; US Bureau of Mines: Chicago, 1978; 110.
5. Perruso, C. R.; Fonseca, M. V. A. Proceedings of the 1st National Symposium on Glasses; March 1995; ACIESP; Vol. 1; p 103.
6. Huggins, M. L.; Sun, K. L.; Silverman, A. J Am Ceram Soc 1943, 26, 393.
7. Wagner, M. P. Rubber Chem Technol 1976, 49, 703.
8. Wason, S. K. in Handbook of Fillers for Plastics; Katz, H. S.; Milewski, J. V.; Eds., Van Nostrand Reinhold: New York, 1987; Chapter 9.
9. Continental, A. G. Eur Rubber J 1995, 177, 53.
10. Legrand, A. P.; Hommel, H.; Tuel, A.; Vidal, A.; Balard, H.; Papirer, E.; Levitz, P.; Czernichowski, M.; Erre, R.; Van Damme, H.; Gallas, J. P.; Hemidy, J. F.; Lavalley, J. C.; Barres, O.; Burneau, A.; Grillet, Y. Adv Colliod Interface Sci 1990, 33, 91.
11. Engelhardt, G.; Michel, D. High-Resolution Solid-State NMR of Silicates and Zeolites; Wiley: New York, 1987.
12. Tuel, A. T.; Hommel, H.; Legrand, A. P.; Chevalier, Y.; Morawski, J. C. Colloids Surf 1990, 45, 413.
13. Iler, R. K. The Chemistry of Silica; Wiley: New York, 1979.
14. Brinker, C. J.; Scherer, G. W. Sol-Gel Science: The Physics and Chemistry of Sol-Gel Processing; Academic Press: New York, 1990.
15. Legrand, A. P.; Taïbi, H.; Hommel, H.; Tougne, P.; Leonardelli, S. J Non-Cryst Solids 1993, 155, 122.
16. Perruso, C. R. D.Sc. Thesis, UFRJ, Rio de Janeiro, 2000.
17. Perruso, C. R. to appear.
18. Brunauer, S.; Emmett, P. H.; Teller, E. J Am Chem Soc 1938, 60, 309.
19. Volf, M. B. Technical Glasses; SNTL: Prague, 1961.
20. Ogunniyi, D. S. Elastomerics 1988, 120, 24.